SENSOR LETTERS
Vol. 1. 93–98, 2003

COMMUNICATION

A New Fiber Optical Thermometer and Its Application for Process Control in Strong Electric, Magnetic, and Electromagnetic Fields

U. Roland,[a,*] C. P. Renschen,[b] D. Lippik,[c] F. Stallmach,[d] and F. Holzer[a]

[a]*UFZ–Centre for Environmental Research Leipzig-Halle, Department of Environmental Technology, Permoserstr. 15, 04318 Leipzig, Germany*
[b]*OPTOcon GmbH, 01309 Dresden, Germany*
[c]*FTZ–Centre for Research and Technology Transfer, 04107 Leipzig, Germany*
[d]*University of Leipzig, Faculty of Physics and Earth Sciences, 04103 Leipzig, Germany*

(Received: 1 September 2003. Revised/Accepted: 8 September 2003)

A new multichannel fiber optical thermometer (FOT) system is described that utilizes the temperature dependence of the band gap of a semiconductor (GaAs). Its modular design allows a flexible multichannel registration and enhances the reliability of the temperature measurement through an innovative sensor concept. The FOT can be easily adapted to a variety of technical and economical requirements, especially those concerning the measuring range, number of channels, accuracy, and cost per channel. Its measuring principle and design make it a versatile tool for utilization under various conditions critical for conventional temperature measurement devices (strong electric and magnetic fields, radio-wave and microwave applications, continuous process monitoring in environmental technology). The examples presented demonstrate the appropriateness, special features, and advantages of the FOT system under microwave and radio-wave irradiation, in a strong electric field and in a very intense static magnetic field in combination with pulsed radio-wave excitation applied in nuclear magnetic resonance spectroscopy. In these cases, the benefits of this multichannel temperature measurement system under *in situ* conditions become apparent.

Keywords: Fiber Optical Thermometer, Electromagnetic Fields, Band Gap, Semiconductor.

The reliable and, in most cases, accurate measurement of temperature is of high importance for a wide variety of technical processes and applications in medicine, engineering, production, and monitoring. Under certain conditions, namely in strong electric, magnetic, and electromagnetic fields (high voltage, radio-wave, and microwave applications, electron spin resonance and nuclear magnetic resonance (NMR) spectroscopy for small-probe testing), in explosive environments, in contact with aggressive media, or for medical applications (NMR tomography), conventional thermocouples or resistance temperature devices such as Pt100 thermometers cannot be used reliably, safely, and without disturbance of the process to be monitored (see, e.g., Ref. 1). For these purposes a number of optical measuring principles are available, based upon the temperature dependence of

- the Raman scattering (ratio of Stokes and anti-Stokes Raman bands),[2]
- relaxation times of fluorescence and luminescence processes,[3] and
- certain properties of solid materials (lattice constant and Bragg angle[4] and position of electronic states in the energy spectrum, particularly the width of the band gap[5, 6]).

Additionally, the emission of light in the infrared or visible range can be exploited to measure the surface temperature of solids or liquids. In this communication, a new fiber

*Corresponding author; E-mail: ulf.roland@ufz.de

  1546-198X/2003/01/093/098/$17.00+.25 doi:10.1166/sl.2003.002

optical thermometer (FOT) is described, together with its application in various fields of science and engineering.

The system records the photon energy sufficient to excite an electron from the valence to the conduction band of a gallium arsenide (GaAs) semiconductor crystal that is mounted on the end of an optical fiber. The required amount of energy is equal to the so-called band-gap energy, E_{gap}. The well-known underlying principle of operation is based on the temperature dependence of the band gap of GaAs (direct [zone center] intrinsic gap; $E_{gap} = 1.423$ eV, corresponding to 872 nm at 300 K; $dE_{gap}/dT = -0.452$ meV/K at 300 K [Ref. 7]). For the FOT application, the spectrum of a GaAs sensor crystal placed in a medium of unknown temperature is measured in the transmission or (diffuse) reflectance mode, and the position of the characteristic edge is analyzed to determine the temperature.

In the patented design for a new, cost-effective, and fast multichannel thermometer[8] based on the above principle, separate temperature measurements of the individual channels are made by switching on the light sources during a defined time interval for only the selected channel while using a single detector for all of them (at least for a set of channels). The backscattering in the optical fiber, which may complicate the evaluation of the spectrum (making the FOT system faulty and susceptible to measurement uncertainties), is reduced by separating the optical fiber pathways routing the light to and from the sensor crystal. A set of optical thermometers has been developed for various purposes with different requirements with respect to number of channels, accuracy, temperature range, and price (FoTemp series from OPTOcon, Dresden, Germany). The main components of a FoTemp-4 are outlined in Figure 1.

The light sources used are either small electric light bulbs (maximum power 1 W) or light-emitting diodes (LEDs) (1A226 from Mitel Semiconductors Tokyo, Japan; emission peak at 900 nm, half-value width approx. 55 nm, optimized for coupling with optical fibers). The light is routed to the sensors via optical fibers (100/110 μm visible/near infrared (VIS/NIR) fibers) that are permanently connected to the sources. The modified spectra of the different channels are transferred to the common evaluation unit (charge-coupled device [CCD] lines with a permanently calibrated optical grating or a commercially available spectrometer [S 2000 from Ocean Optics Inc.; 100-μm slit]) designed for measurement in a typical wavelength range of 850 to 1100 nm via an optical mixer. This mixing unit consists of a light-scattering polymer and is usually made spherical with a diameter of about 10 mm. Interrogation of the individual measuring channels is accomplished by the time-staggered triggering of the corresponding light sources and suitable evaluation of the detector signal. Typically, four channels are combined into one optical block with integrated data acquisition and processing. This modular construction concept significantly reduces susceptibility to various disturbances.

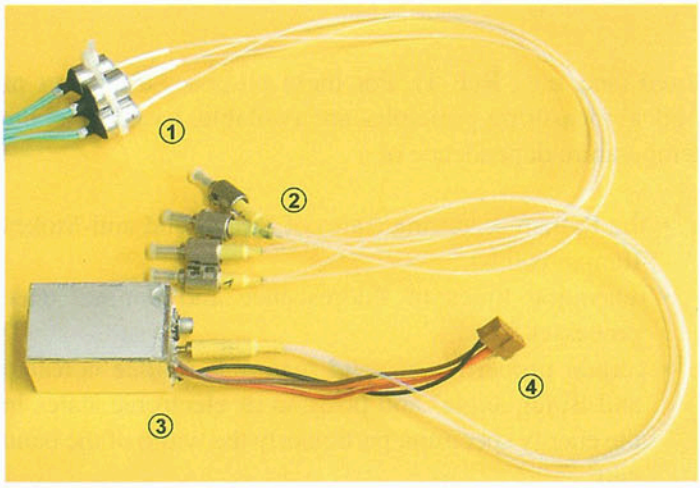

Figure 1. Principal components of a modular four-channel FoTemp-4 fiber optical thermometer: **1**, light sources; **2**, ST connectors with integrated optical coupling; **3**, spectral detection unit (with CCD line and optical grating); and **4**, electronic interface.

The optical fibers connecting the GaAs sensor crystal with the light source and the detector in the evaluation unit, respectively, may have a length of up to several hundred meters. Two different types are used, where either a long or a short part of the optical fibers for light routing to and from the sensor crystal is separated. All probes are completely nonmetallic: the fiber material is polyimide-coated silica, and the sensor crystal at the tip (GaAs, fixed with a temperature-resistant adhesive) is covered with polytetrafluoroethylene (PTFE) (Teflon). The diameter of the tip is about 1.5 mm. A second advantage in addition to its small size is the low heat capacity of the sensor, preventing a significant disturbance of the system to be measured (whether in a gaseous, liquid, or solid state) and making the measurement fast. The sensor is connected with the thermometer by conventional ST (straight tip) or other user-specific connectors. Depending on the type of sensor and instrumentation, the measuring range is from −50 °C to 300 °C. After appropriate multipoint calibration, an accuracy of 0.1 K can be achieved with the use of an adequate CCD line. However, a low-cost version with 3 K system accuracy is available for monitoring tasks (e.g., with high-power transformers or electric motors). The measuring time per channel can be varied from about 100 ms to several seconds. Because of the block-wise construction, a quasi-parallel measurement mode can be applied for multichannel FoTemp thermometers. An automatic internal calibration procedure is applied for each individual channel to optimize the integration time related to the temperature, the sensor properties (including their lengths), and the sensitivity of the detector. Some components of the optical thermometer shown in Figure 1 (detector, sensor design, optical coupling) may vary, depending on the FoTemp type.

In addition to its heat capacity, the heat conductivity of a temperature sensor is an important property that controls the degree of interference with the original temperature profile to be measured. Because of the use of optical fiber connections, the FOT sensors have a minimal impact on the surrounding medium.

In the following, some test measurements under "critical" conditions and applications of the FOT in environmental technology will be presented without a discussion of the results of the specific investigations in detail.

One of the motivations to develop the FoTemp thermometers was the necessity to measure small temperature differences during environmental studies dealing with seasonal changes, influences of dielectric heating with radiowaves on soil cleaning, and microbiological processes at elevated temperatures.[9] In Figure 2, the temperature course in a soil reactor used for microbiological decontamination is compared for optical (different integration times) and conventional measurements showing that differences of 0.1 K can be monitored with adequate instrumentation.

The phase transition of suitable media can be used to calibrate the temperature or check the accuracy in a convenient manner. The transfer of the melting heat or the heat of evaporation to the system to be heated usually corresponds to a stabilization of the temperature at the melting or vaporization point, respectively, for a certain time. As an example, microwave heating of ice in a household oven (maximum power 900 W) up to the evaporation of water is shown in Figure 3. The expected temperature plateaus at 0 °C and 100 °C indicate the accuracy of the measurement by the FoTemp-8 thermometer. As is characteristic for dielectric heating (using frequencies in the microwave as well as in the radio-wave range from MHz to GHz), the energy absorption of the liquid phase is larger than in the ice, leading to a significant overheating of the water. This effect is due to the different dielectric losses (imaginary part of the relative dielectric constant) of the components.

The dependence of the melting point of confined water on the pore size is used to characterize porous materials by cryoporometry.[10] To distinguish between the states of aggregation, several thermal and spectroscopic methods can be applied. The utilization of one such method, NMR spectroscopy, is described later in this communication.

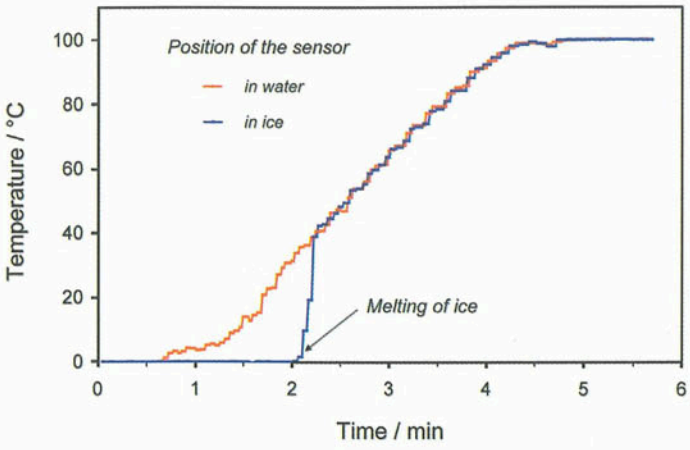

Figure 3. Stabilization of the temperature due to melting of ice and evaporation of water at 0 °C and 100 °C, respectively, as measured by a FoTemp-8 thermometer during heating in a microwave oven (pulsed microwave application, 900 W; temperature measurement every 1 s).

The oxidation of hazardous volatile organic compounds (VOCs) in an electrical discharge, a so-called nonthermal plasma (NTP), is a relatively new method for cleaning contaminated gas streams.[11, 12] Because of the nonequilibrium conditions ("hot" electrons with a kinetic energy corresponding to about 10^4 K; neutral gas molecules remain nearly cold), this method is expected to achieve a high energetic efficiency, especially for low VOC concentrations. Under these conditions, conventional thermal and thermocatalytic methods do not work effectively. Recently, the combination of NTP and catalytic processes has been tested with the use of a barrier reactor (described in detail in Ref. 11; discharge gap of 5 mm in a coaxial-electrode reactor, applied voltage up to 35 kV, basic frequency 50 Hz). The FOT was successfully used to measure the temperature in the discharge zone. No influence of the strong electric field in the NTP discharge zone was observed (Figure 4). As expected, the gas temperature in the nonthermal plasma is not significantly higher than that at

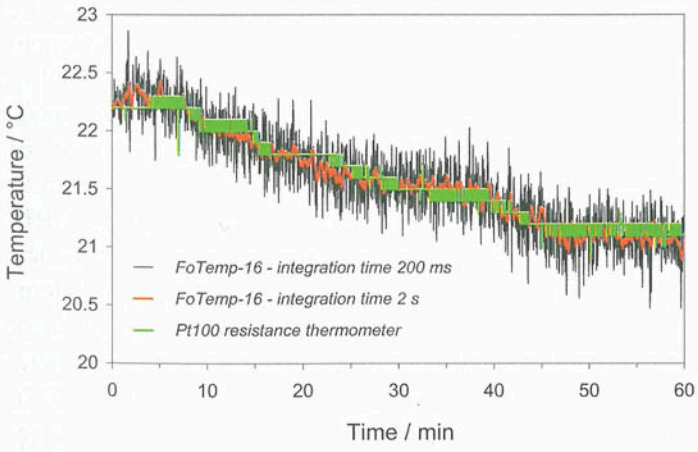

Figure 2. Temperature development in the upper part of an open soil compartment as measured either by a FoTemp optical thermometer with two different integration times (200 ms and 2 s) or by a conventional Pt100 resistance thermometer.

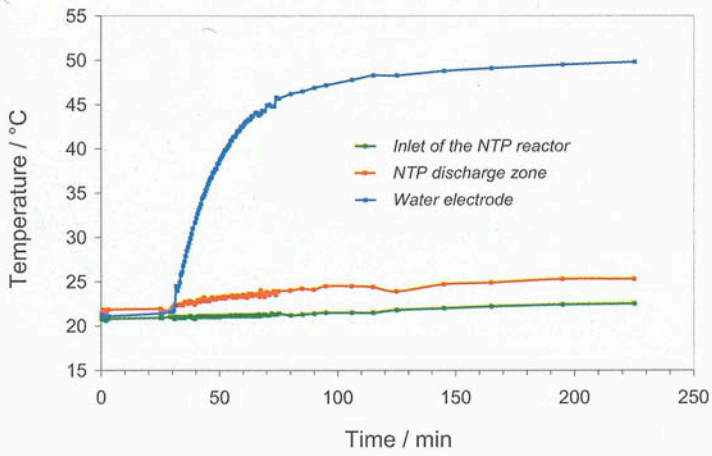

Figure 4. Temperatures in the discharge zone of a nonthermal plasma, at the inlet of the plasma reactor, and in the water electrode as a function of time (coaxial barrier discharge reactor,[11] applied voltage 15 kV, basic frequency 50 Hz, air flow 78 ml/min, residence time 9.2 s).

the inlet of the NTP reactor. In contrast, a marked heating occurs in the water used as the outer electrode of the coaxial glass-barrier arrangement.

The temperature plays an important role for many parameters and processes relevant to the remediation of contaminated soils and other materials. Thus, the microbiological degradation rates are optimal at about 35 °C for most microorganisms. The water solubilities, vapor pressures and mobilities of the pollutants are enhanced by heating the medium above ambient temperature. This is a central feature of several technologies, such as thermally enhanced soil vapor extraction. Radio-wave (dielectric) heating is a unique method for producing temperature changes in the soil in a wide range up to more than 400 °C, under *in situ*, *ex situ*, and on-site conditions and for many materials (dry and humid, sandy and tenacious soils).[9] Continuous temperature monitoring by optical sensors is an essential prerequisite for an effective process control. At a field site for thermally enhanced microbiological remediation of soils (Figure 5; HF power source IS 15 from Hüttinger Elektronik, Freiburg/Brsg., Germany; maximum RF power 15 kW, frequency 13.56 MHz) contaminated with organic compounds, about 50 fiber optical temperature sensors have been applied to measure soil heating in a reactor with a size of $3 \times 3\ m^2$ (1 m depth). For example, the temperature profiles in the horizontal planes at four different heights are shown in Figure 6. The sufficiently homogeneous temperature distribution in the stationary period of the remediation (constant T) demonstrates the appropriateness of the system for radio-wave heating, including the temperature measurement avoiding, for example, significant overheating, which would reduce the number of microbes. The RF method has been successfully tested in long-term experiments (lasting several months) for thermally enhanced bioremediation as well as soil vapor extraction.[9] It is expected to be especially effective under conditions where ambient

Figure 5. Soil reactor with electromagnetic shielding for thermally enhanced biodegradation of contaminants via radio-frequency dielectric heating (bioremediation facility of Bauer & Mourik Umwelttechnik in Hirschfeld, Germany).

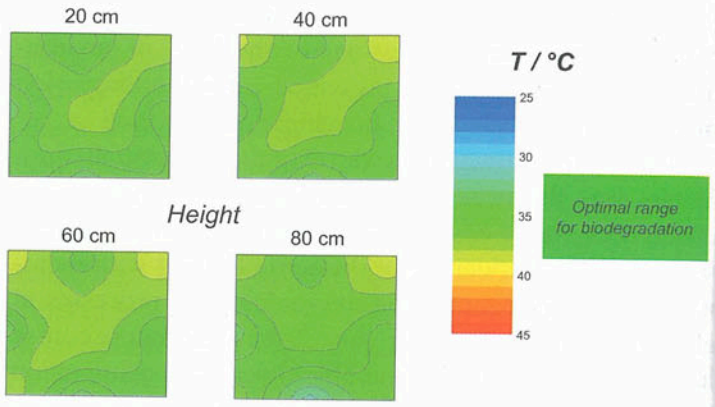

Figure 6. Temperature profiles in the soil reactor after radio-wave heating to an optimum temperature of approx. 35 °C during a long-term investigation of stimulated biodegradation (at four different heights) as measured by a FOT.

temperatures are low or when remediation times have to be kept short.

The characterization of liquid phases, especially water, in natural materials such as rocks, sands, and soils is of great importance not only in geology (e.g., during prospecting for oil and other raw materials) but also in environmental science and technology (remediation of contaminated soil). When radio-wave heating is used under cold climatic conditions (permafrost) to mobilize the contaminants and stimulate biodegradation, the state (frozen or melted) and allocation of water must be determined to avoid an unwanted mobilization of pollutants. ^{1}H NMR spectroscopy is a suitable tool for studying the ice-water transition under various conditions (soil material, porosity, and pore size distribution). The method uses the freezing point depression of water with decreasing pore size (Kelvin law) and the large differences in transverse (T_2) nuclear magnetic relaxation time between liquid water and solid ice in the pore system. In particular, pore size distributions can be determined by analyzing the relative amount of the liquid water phase as a function of temperature (NMR cryoporometry[10]).

To use the FoTemp thermometer in the low-temperature range, it must be multipoint calibrated because the dependence of E_{gap} on the temperature becomes more nonlinear.[7] Additionally, the strong magnetic fields used in modern NMR spectrometers (up to 19 T) cause small shifts of the band-gap width of GaAs (compare Ref. 13). In our experiments with a home-built NMR spectrometer (FEGRIS 400 NT equipped with a Bruker Spectrospin superconducting [sc] magnet, ^{1}H resonance frequency 400 MHz; temperature control of the NMR sample by a stream of air or nitrogen with known temperature[14]), a static magnetic field of $B_0 = 9.4$ T led to an apparent temperature shift of about 5 K, as recorded with the FoTemp FOT without recalibration. This effect and, as a typical example, the temperature values obtained after a normal calibration procedure was carried out (two-point calibration at 30 °C and 60 °C) are presented in Table I.

Table I. Measured temperatures after two-point calibration (reference temperature determined by Hg thermometer) of a FoTemp-16 thermometer at 30 °C and 60 °C outside and inside a strong magnetic field with and without recalibration.

T_{Ref} (°C) $B = 0$	T_{FoTemp} (°C) $B = 0$	T_{FoTemp} (°C) $B = 9.4T$ before recalibration	T_{FoTemp} (°C) $B = 9.4T$ after recalibration	ΔT (K) T shift in B without recalibration
25.0	25.2	20.6	25.1	4.5
30.0	29.9	25.4	29.9	4.5
40.0	39.6	35.3	39.7	4.4
60.0	59.6	55.5	60.0	4.5

In Figure 7, the increase in the sample temperature as measured by a fiber optical thermometer (FoTemp-16) is shown after the temperature of the nitrogen flow around the sample (measured by a Pt100 thermometer outside the radio-frequency [rf] coil of the NMR spectrometer) was raised from −5 °C to −2 °C and then to 2 °C. The sample consisted of sand with a grain size ranging from 125 to 180 μm and a water content approx. 60% of the pore volume. The temperature change in the gas flow occurs within about 20 s, and the temperature increase in the sample reflects the heat transfer kinetics and, as can be seen from the plateau at 0 °C, the melting of the ice mainly present in the interparticle space (phase-transition point). As shown in Figure 8, this process can also be observed with the NMR relaxation time T_2 measured with the CPMG[15] NMR pulse sequence, which detects and analyzes the intensities of a series of spin echoes (echo spacing 240 μs) arising after a pulsed rf excitation of the proton nuclear spins of the water. The rf pulses did not interfere with the FoTemp temperature measurements, although the sensor was placed in the center of the sample volume and, thus, in the center of the rf field. The liquid phase in the volume between the sand grains (characterized by relatively long T_2 values of about 5 to 15 ms) dominates at $T >$ 0 °C, whereas the short T_2 for ice is observed at $T = -2$ °C.

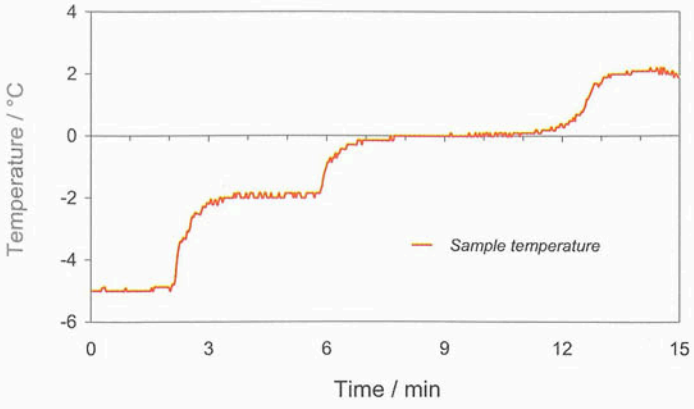

Figure 7. Development of the temperature measured directly in an initially frozen sample (sand with a water content approx. 60% of the pore volume) after the temperature of the surrounding gas flow was increased from −5 °C to −2 °C (after 2.1 min) and from −2 °C to 2 °C (after 5.8 min; each heating step within about 20 s).

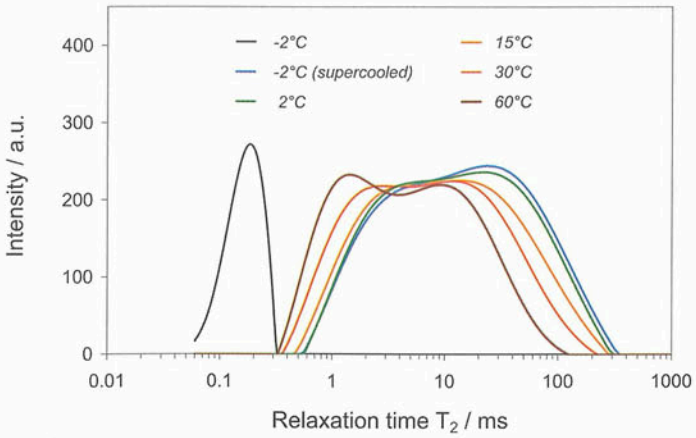

Figure 8. Distribution of NMR relaxation times T_2 of a humid sand sample (water content approx. 60% of the pore volume) as a function of temperature continuously measured by a FoTemp FOT placed in the center of a sand/water sample in an NMR coil.

The wide relaxation time distribution between the melting point and 60 °C is typical for liquid water between sand grains.[16] Because of a decreasing self-diffusion coefficient of liquid water with decreasing temperature, the center of gravity of the T_2 distribution is shifted to larger relaxation times. A special case is supercooled liquid at a temperature slightly below the freezing point, which shows the NMR relaxation time typical for liquid water (Figure 8). In this state, slight mechanical vibration of the NMR sample holder initiated the freezing process of water between the sand grains. The melting heat that is released during freezing increases the temperature in the center of the sample to 0 °C, as measured by the FOT, although the stream of nitrogen outside the sample is kept at −2 °C. Such processes, of course, could not be followed by conventional thermometers because the space in the NMR sample volume needs to be free of any electrically conducting material (wires, metals) because of its disturbing influences on the (pulsed) rf field.

The *in situ* applications of the FoTemp FOT in the various fields briefly described here demonstrate its suitability for (continuous) temperature measurement under conditions where conventional temperature monitoring usually fails.

References and Notes

1. E. Pert, Y. Carmel, A. Birnboim, T. Olorunyolemi, D. Gershon, J. Calame, I. K. Lloyd, and O. C. Wilson, Jr., *J. Am. Ceram. Soc.* 84, 1981 (**2001**).
2. J. P. Dakin, D. J. Pratt, G. W. Bibby, and J. N. Ross, *Electron.Lett.* 21, 569 (**1985**).
3. M. H. Sun and A. Kamal, *SPIE Ser. Opt. Fibres Med. VI* 1420, 44 (**1991**).
4. S. M. Melle, K. Liu, and R. Measures, *Appl. Opt.* 32, 3601 (**1993**).
5. Y. Zhao and Y. Liao, *Opt. Commun.* 215, 11 (**2003**).
6. P. C. Russell, R. Haber, G. R. Jones, and W. McGrory, *Sens. Actuators* 76, 231 (**1999**).
7. J. S. Blakemore, *J. Appl. Phys.* 53, R123 (**1982**).
8. C. P. Renschen and U. Roland, German Patent DE 10027533 (**2001**).
9. U. Roland, F.-D. Kopinke, F. Holzer, R. Blechschmidt, and P. Harting, in *Contaminated Soil 2003, Proceedings of the Eighth International*

FZK/TNO Conference on Contaminated Soil, F & U confirm, Leipzig (**2003**), p. 1885.
10. J. H. Strange, J. Mitchell, and J. B. W. Webber, *Magn. Res. Imaging* 21, 221 (**2003**).
11. F. Holzer, U. Roland, and F.-D. Kopinke, *Appl. Catal., B* 38, 163 (**2002**).
12. M. Kraus, B. Eliasson, U. Kogelschatz, and A. Wokaun, *Phys. Chem. Chem. Phys.* 3, 294 (**2001**).
13. L. Bryja, O. Stern, M. Kubisa, K. Ryczko, M. Bayer, J. Misiewicz, A. Forchel, and O. P. Hansen, *Thin Solid Films* 380, 142 (**2000**).
14. P. Galvosas, F. Stallmach, G. Seiffert, J. Kärger, U. Kaess, and G. Majer, *J. Magn. Reson.* 151, 260 (**2001**).
15. H. Y. Carr and E. M. Purcell, *Phys. Rev.* 94, 630 (**1954**).
16. C. Vogt, P. Galvosas, N. Klitzsch, and F. Stallmach, *J. Appl. Geophys.* 50, 455 (**2002**).